



ChemComm

**Evidence for a Lowest Energy 3MLCT Excited State in  
[Fe(tpy)(CN)<sub>3</sub>]<sup>-</sup>**

Journal:	<i>ChemComm</i>
Manuscript ID	CC-COM-02-2021-001090.R1
Article Type:	Communication

SCHOLARONE™  
Manuscripts

## COMMUNICATION

Evidence for a Lowest Energy <sup>3</sup>MLCT Excited State in [Fe(tpy)(CN)<sub>3</sub>]<sup>-</sup>

Received 00th January 20xx,  
Accepted 00th January 20xx

Sebastian B. Vittardi,<sup>a</sup> Rajani Thapa Magar,<sup>a</sup> Briana R. Schrage,<sup>†c</sup> Christopher J. Ziegler<sup>†c</sup>, Elena Jakubikova<sup>†b</sup> and Jeffrey J. Rack<sup>†‡a</sup>

DOI: 10.1039/x0xx00000x

**Transient absorption data of [Fe<sup>II</sup>(tpy)(CN)<sub>3</sub>]<sup>-</sup> reveals spectroscopic signatures indicative of <sup>3</sup>MLCT with a ~10 ps kinetic component. These data are supported by DFT and TD-DFT calculations, which show that excited state ordering is responsive to the number of cyanide ligands on the complex.**

There is considerable interest in the replacement of ruthenium by iron in a variety of transition metal chromophores. Much of this effort is aimed at “making iron the new ruthenium,” with the ultimate goal of many of these studies to create a long-lived <sup>3</sup>MLCT state (Metal-to-Ligand Charge-Transfer) through judicious choice of ligand and solvent environment.<sup>1</sup> While the formation of this state in ruthenium polypyridine chemistry is straightforward and requires little special effort, it has been found by many researchers that the lowest energy excited states of many iron chromophores is Ligand Field (LF) or Metal-Centered (MC) in character, and thus the excited states are neither long-lived nor of appropriate energy to perform one-electron oxidation or reduction chemistry.<sup>2</sup> For example, Winkler, Creutz, and Sutin reported that while [Fe(bpy)<sub>3</sub>]<sup>2+</sup> and [Fe(bpy)<sub>2</sub>(CN)<sub>2</sub>] featured lowest energy excited states that were LF in nature, that only in the presence of a weak acceptor solvent (acetone), could an MLCT excited state in [Fe(bpy)(CN)<sub>4</sub>]<sup>2-</sup> be observed.<sup>3</sup> This result has been confirmed by a variety of researchers and a variety of techniques. Many of these studies have focused on [Fe(bpy)<sub>2</sub>(CN)<sub>2</sub>] and [Fe(bpy)(CN)<sub>4</sub>]<sup>2-</sup> as well as [Fe(bpy)<sub>3</sub>]<sup>2+</sup> and [Fe(CN)<sub>6</sub>]<sup>3-</sup> within a comparative series.<sup>4-16</sup>

An omission from this series is [Fe(tpy)(CN)<sub>3</sub>]<sup>-</sup>, and we questioned if the balance of ligand field strength and CT energy were such that an MLCT state might be accessible or even lowest in energy in this complex. DFT and TD-DFT

calculations on series of Fe(II) polypyridine complexes with a systematically increasing number of CN<sup>-</sup> ligands ([Fe(bpy)<sub>3</sub>]<sup>2+</sup>, [Fe(bpy)<sub>2</sub>(CN)<sub>2</sub>], [Fe(tpy)(CN)<sub>3</sub>]<sup>-</sup>, [Fe(bpy)(CN)<sub>4</sub>]<sup>2-</sup>) suggest that this may be the case. Figure 1 shows the calculated energies of the relevant electronic states of the Fe(II) complexes in Franck-Condon region. As can be seen here, the energies of the <sup>1,3</sup>MLCT states (shown in blue and purple in Figure 1) become stabilized with the increasing number of CN<sup>-</sup> ligands bound to the Fe(II) center. At the same time, the energy of the lowest-lying <sup>5</sup>MC state increases significantly, with the <sup>1,3</sup>MLCT states becoming more stable than the <sup>5</sup>MC state for [Fe(tpy)(CN)<sub>3</sub>]<sup>-</sup>. This suggests a possible presence of low-lying <sup>3</sup>MLCT states for this complex. Although DFT calculations often struggle to reproduce the correct ordering of electronic states with different spins,<sup>17-18</sup> the systematic behaviour observed in Figure 1 was compelling enough for us to synthesize [Fe(tpy)(CN)<sub>3</sub>]<sup>-</sup> complex and measure its photophysical properties.

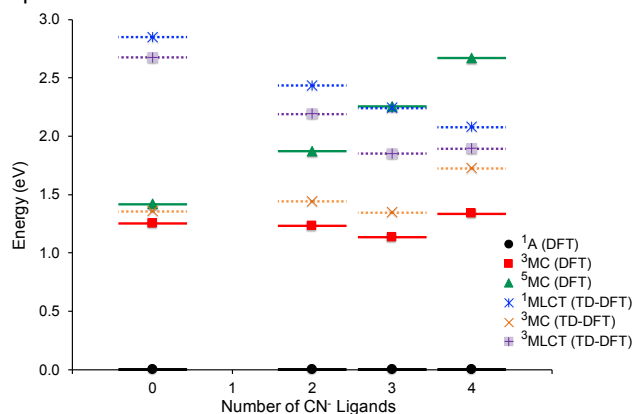


**Figure 1.** Calculated energies of relevant electronic states for [Fe(bpy)<sub>3</sub>]<sup>2+</sup> (0 CN<sup>-</sup> ligands), [Fe(bpy)<sub>2</sub>(CN)<sub>2</sub>] (2 CN<sup>-</sup> ligands), [Fe(tpy)(CN)<sub>3</sub>]<sup>-</sup> (3 CN<sup>-</sup> ligands), and [Fe(bpy)(CN)<sub>4</sub>]<sup>2-</sup> (4 CN<sup>-</sup> ligands) in Franck-Condon region. Only the structure of <sup>1</sup>A (ground state) was fully optimized, energies of the other electronic states were obtained either from the single-point energy calculations (DFT) at the <sup>1</sup>A optimized geometry, or from TD-DFT calculations with <sup>1</sup>A as the reference state.

The tricyano complex is readily prepared through reaction of [Fe(tpy)Cl<sub>2</sub>] with an excess of KCN in boiling water (Scheme S1, ES†).<sup>8</sup> Crystals suitable for X-ray diffraction were grown from ethanol solution, ultimately yielding the structure shown in

<sup>a</sup> Department of Chemistry and Chemical Biology, University of New Mexico, Albuquerque, NM 87131.

<sup>b</sup> Department of Chemistry, North Carolina State University, Raleigh, NC 27695

<sup>c</sup> Knight Chemical Laboratory, Department of Chemistry, University of Akron, Akron, OH.

<sup>†</sup> Authors to whom correspondence should be addressed.

Electronic Supplementary Information (ESI) available: CCDC 2058114 contains the supplementary crystallographic data for this paper. See DOI: 10.1039/x0xx00000x

Figure 2, with an expected meridional geometry of the three cyano ligands. The axial Fe–C bonds are 1.939(1) and 1.951(1) Å, with the remaining equatorial Fe–C bond exhibiting the shortest distance of 1.909(1) Å. There are no significance differences in the C–N bond lengths of the cyano groups. The Fe–N bond distances are typical for terpyridine coordination, with the central Fe–N bond distance (1.883(1) Å) being shorter than the Fe–N bond distances for the peripheral pyridines (1.969(1) Å and 1.966(1) Å).<sup>19–24</sup> We note that these distances are also consistent with low spin iron electron configuration.

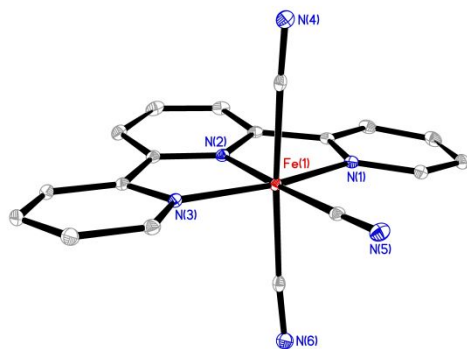


Figure 2. Molecular structure of  $[\text{Fe}(\text{tpy})(\text{CN})_3]^-$  rendered with 35% thermal ellipsoids.  $\text{K}^+$  ions and H atoms not shown for clarity. Color scheme: Fe, red; C, grey; N, blue.

The  $^1\text{H}$  NMR spectra and infrared spectrum are consistent with the molecular structure (Figures S1 – S5 and Tables S1 – S2, ESI<sup>†</sup>). Specifically, the infrared spectrum features three  $\nu(\text{CN})$  at 2091, 2069 and 2060  $\text{cm}^{-1}$ . These compare well with  $[\text{Fe}(\text{bpy})_2(\text{CN})_2]$  where  $\nu(\text{CN})$  is 2072  $\text{cm}^{-1}$  and  $[\text{Fe}(\text{bpy})(\text{CN})_4]^{2-}$  where  $\nu(\text{CN})$  is 2032, 2044, 2057, and 2083  $\text{cm}^{-1}$ . As all three complexes are  $\text{C}_2$  (or  $\text{C}_{2v}$ ) symmetric, each CN should be uniquely identified in the infrared spectrum. The absence of a definitive peak for the dicyano complex suggests that it is underneath the intense asymmetric  $\nu(\text{CN})_2$  peak at 2072  $\text{cm}^{-1}$ . The experimental UV-vis spectrum is shown in Figure 2A and the calculated spectrum is shown in Figure S4 (ESI<sup>†</sup>). The calculated spectrum reproduces well the features found in the experimental spectrum and analysis reveals that the lowest energy visible transitions are primarily MLCT in character with some MC character (Table S3, ESI). Similar to the tetracyano complex ( $[\text{Fe}(\text{bpy})(\text{CN})_4]^{2-}$ ),  $[\text{Fe}(\text{tpy})(\text{CN})_3]^-$  features two broad MLCT absorptions in the visible, but the lowest energy CT band for the tpy complex is quite broad, extending to 850 nm. In accord with many cyano complexes, the tricyano complex is strongly solvatochromic with the intensity, wavelength and shape all strongly dependent upon the choice of solvent (Figure S6, ESI<sup>†</sup>).<sup>3, 5, 7, 25</sup> Indeed, the lowest energy maximum is observed at 497 nm in  $\text{H}_2\text{O}$ , at 530 nm in  $\text{CH}_3\text{OH}$ , and at 668 nm in  $\text{CH}_3\text{CN}$ . Lastly, we note that cyclic and square wave voltammetry reveals a  $\text{Fe}^{3+/2+}$  couple of 0.17 V vs Ag wire in propylene carbonate.

We employed femtosecond transient absorption spectroscopy

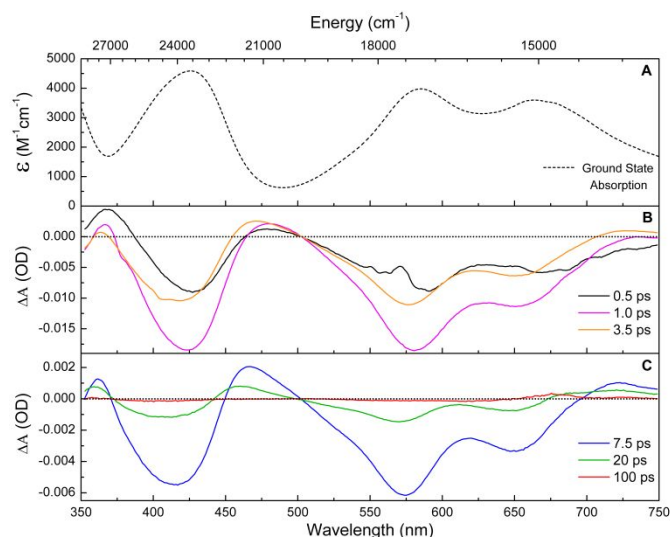


Figure 3. Ground state UV-Vis spectrum of  $\text{K}[\text{Fe}^{\text{II}}(\text{tpy})(\text{CN})_3]$  (A) in acetonitrile. Selected excited state spectra at early (B) and late (C) pump-probe time delays in acetonitrile. The legend details the exact pump-probe time delay for each spectrum.

to determine whether or not  $[\text{Fe}(\text{tpy})(\text{CN})_3]^-$  exhibits evidence for an MLCT excited state following excitation. Spectral features consistent with an MLCT typically include an excited state absorption that is ascribed to a reduced bpy  $\pi^* \rightarrow \pi^*$  transition near 370 nm, and an unreduced bpy  $\pi \rightarrow \text{Fe}^{\text{III}}$  LMCT transition in the red portion of the spectrum.<sup>11</sup> LF or MC lowest energy excited states do not typically feature any excited state absorption at any wavelength (See Figure S7, ESI<sup>†</sup> for data on  $[\text{Fe}(\text{bpy})_2(\text{CN})_2]$  and  $[\text{Fe}(\text{bpy})(\text{CN})_4]^{2-}$ ).<sup>26</sup> Shown in Figure 3 (B and C) are transient spectra of  $[\text{Fe}(\text{tpy})(\text{CN})_3]^-$  collected at different pump-probe time delays. The first trace (0.5 ps; black) shows a transient that nicely mirrors the ground state absorption spectrum and features negative absorbances or bleaches with maxima that correspond well with the ground state absorption (Figure 3A). However, excited state absorptions are apparent at both  $\sim 350$  nm and  $\sim 475$  nm. From 0.5 ps to 1 ps, the bleach features become more intense (grow more negative) as does the excited state absorption near  $\sim 475$  nm. Also during this time, the long wavelength bleach feature narrows, yielding to a small excited state absorption at  $\sim 750$  nm, reminiscent of what is observed in the transient spectra of  $[\text{Fe}(\text{bpy})(\text{CN})_4]^{2-}$ .<sup>5, 11, 25</sup> During this time interval, the peak maxima all shift to the blue, perhaps suggesting that this process is dominated by vibrational cooling, but may also be simply due to the last vestiges of  $^3\text{MLCT}$  formation. From 1 ps to 20 ps, the bleach maxima continue to shift blue, but lessen in intensity, ultimately relaxing to a transient that is indistinguishable from the zero line at 100 ps pump probe time delay. The excited state absorption at  $\sim 475$  nm first rises in intensity and then relaxes back to the zero line, while the excited state absorption at  $\sim 350$  nm broadens and loses intensity over this time interval. Lastly, the emergent excited state absorption at  $\sim 750$  nm gains intensity while moving to the blue, before ultimately relaxing to the zero line. As the transient absorption signal is always the sum of multiple contributions (e.g., ground state bleach, excited state absorption, among others), we are

cautious not to over-interpret the shifting of excited state absorptions or their band shape, as band shape variations could be due to changes in the bleach regions, which are dominant in the spectrum. Nevertheless, we do interpret the presence of excited state absorptions throughout the entirety of the transient absorption experiment as evidence for the formation of a lowest energy MLCT excited state in  $[\text{Fe}(\text{tpy})(\text{CN})_3]^-$ . Consistent with our global fitting results, single wavelength kinetic analysis retrieved from 550 nm yielded time constants of  $2.9 \pm 0.5$  ps and  $9.5 \pm 0.6$  ps (Figure S8, ESI<sup>†</sup>). In accord with our discussion above, we assign the short time constant to intramolecular vibrational energy redistribution, and the long time constant to relaxation of the  $^3\text{MLCT}$  to the ground state. These assignments are consistent with those made for related complexes (see below).

The excited state lifetime of  $[\text{Fe}(\text{tpy})(\text{CN})_3]^-$  ( $\tau$   $9.5 \pm 0.6$  ps) is in accord with  $[\text{Fe}(\text{bpy})_2(\text{CN})_2]$  ( $\tau$  330 ps<sup>27</sup> or  $256 \pm 4$  ps<sup>6</sup>) and  $[\text{Fe}(\text{bpy})(\text{CN})_4]^{2-}$  ( $\tau$   $2.5 \pm 0.$  ps and  $\tau$   $18.5 \pm 0.9$  ns).<sup>11</sup> Similar to  $[\text{Fe}(\text{bpy})_2(\text{CN})_2]$  and  $[\text{Fe}(\text{bpy})(\text{CN})_4]^{2-}$ , we find no evidence of photodecomposition in  $[\text{Fe}(\text{tpy})(\text{CN})_3]^-$ , which has been observed in  $[\text{Fe}^{\text{II}}(\text{py})(\text{CN})_5]^{n-}$ , where py is a substituted pyridine.<sup>28</sup> Gaffney, Kjaer and coworkers ascribe the 2.5 ps lifetime in their study of  $[\text{Fe}(\text{bpy})(\text{CN})_4]^{2-}$  to intramolecular vibrational energy redistribution and solvent dynamics, and specifically state that this kinetic phase is not assigned to excited electronic state dynamics based on a combination of XAS and visible femtosecond pump probe date.<sup>11</sup> In contrast to what was reported for  $[\text{Fe}(\text{bpy})(\text{CN})_4]^{2-}$ , our data do not unequivocally indicate if  $^1\text{A}_1$  ground state occurs directly from the  $^3\text{MLCT}$  state or if there is an intervening state (LF) that facilitates excited state deactivations.

The computational results displayed in Figure 1 refer to electronic state ordering near the Franck-Condon region following excitation. At present, we are uncertain of the relative ordering as the molecule moves away from this region, towards the lowest energy excited state, yet the spectroscopic data presented here suggest that the  $^3\text{MLCT}$  is lowest, or at least kinetically favoured over the MC states. For example, an Fe(II) *N*-heterocyclic carbene complex displays a long-lived  $^3\text{MLCT}$  state, despite the fact that the  $^3\text{MC}$  state is thermodynamically favoured.<sup>29</sup> Recent computational data on  $[\text{Fe}(\text{tpy})_2]^{2+}$  suggest the importance of a rocking motion,<sup>30</sup> and others identify the significance of bond lengthening during excited state evolution and deactivation.<sup>31</sup> We speculate that the dynamical motions of the terpyridine in combination with the vibrations associated with three cyanide ligands in  $[\text{Fe}(\text{tpy})(\text{CN})_3]^-$ , not only conspire to stabilize the  $^3\text{MLCT}$  state, but also facilitate coupling to the ground state  $^1\text{A}$  surface, such that the excited state lifetime is significantly shorter than that observed for  $[\text{Fe}(\text{tpy})_2]^{2+}$  ( $\tau$   $5.2 \pm 0.1$  ns). Further studies on related complexes will hopefully reveal these and other details.

## Conclusion

The data presented here strongly support the assignment of the lowest energy excited state to  $^3\text{MLCT}$  for  $[\text{Fe}(\text{tpy})(\text{CN})_3]^-$ .

Specifically, the appearance of excited state absorptions in the transient spectra provides compelling evidence for this assignment. The study presented here completes the comparative series of iron complexes containing polypyridine and cyanide ligands, and suggest that other small ligands coordinated to  $[\text{Fe}(\text{tpy})]^{2+}$  may ultimately lead to a longer lived  $^3\text{MLCT}$  state.

## Conflicts of interest

There are no conflicts to declare.

## Notes and references

‡ JJR acknowledges financial support from the National Science Foundation (CHE 1856492) and the Army Research Laboratory (W911NF-19-2-0175).

§ EJ gratefully acknowledges the support from the U.S. Army Research Office under the contract W911NF-19-2-0194.

1. Wenger, O. S., Is Iron the New Ruthenium? *Chem.-Eur. J.* **2019**, *25* (24), 6043-6052.
2. McCusker, J. K., Electronic structure in the transition metal block and its implications for light harvesting. *Science* **2019**, *363* (6426), 484-488.
3. Winkler, J. R.; Creutz, C.; Sutin, N., SOLVENT TUNING OF THE EXCITED-STATE PROPERTIES OF (2,2'-BIPYRIDINE)TETRACYANOFERRATE(II) - DIRECT OBSERVATION OF A METAL-TO-LIGAND CHARGE-TRANSFER EXCITED-STATE OF IRON(II). *J. Am. Chem. Soc.* **1987**, *109* (11), 3470-3471.
4. Jay, R. M.; Eckert, S.; Fondell, M.; Miedema, P. S.; Norell, J.; Pietzsch, A.; Quevedo, W.; Niskanen, J.; Kunnus, K.; Fohlisch, A., The nature of frontier orbitals under systematic ligand exchange in (pseudo-)octahedral Fe(II) complexes. *Phys. Chem. Chem. Phys.* **2018**, *20* (44), 27745-27751.
5. Kjaer, K. S.; Kunnus, K.; Harlang, T. C. B.; Van Driel, T. B.; Ledbetter, K.; Hartsock, R. W.; Reinhard, M. E.; Koroidov, S.; Li, L.; Laursen, M. G.; Biasin, E.; Hansen, F. B.; Vester, P.; Christensen, M.; Haldrup, K.; Nielsen, M. M.; Chabera, P.; Liu, Y. Z.; Tatsuno, H.; Timm, C.; Uhlig, J.; Sundstom, V.; Nemeth, Z.; Szemes, D. S.; Bajnoczi, E.; Vanko, G.; Alonso-Mori, R.; Glowina, J. M.; Nelson, S.; Sikorski, M.; Sokaras, D.; Lemke, H. T.; Canton, S. E.; Warnmark, K.; Persson, P.; Cordones, A. A.; Gaffney, K. J., Solvent control of charge transfer excited state relaxation pathways in Fe(2,2'-bipyridine)(CN)(4) (2-). *Phys. Chem. Chem. Phys.* **2018**, *20* (6), 4238-4249.
6. Kjaer, K. S.; Zhang, W. K.; Alonso-Mori, R.; Bergmann, U.; Chollet, M.; Hadt, R. G.; Hartsock, R. W.; Harlang, T.; Kroll, T.; Kubicek, K.; Lemke, H. T.; Liang, H. Y. W.; Liu, Y. Z.; Nielsen, M. M.; Robinson, J. S.; Solomon, E. I.; Sokaras, D.; van Driel, T. B.; Weng, T. C.; Zhu, D. L.; Persson, P.; Warnmark, K.; Sundstrom, V.; Gaffney, K. J., Ligand manipulation of charge transfer excited state relaxation and spin crossover in Fe(2,2'-bipyridine)(2)(CN)(2). *Struct. Dyn.-US* **2017**, *4* (4), 11.
7. Moya, M. L.; Rodriguez, A.; Sanchez, F., SPECIFIC CATION SOLUTE INTERACTIONS AS A MAJOR CONTRIBUTOR TO THE SALT EFFECTS ON CHARGE-TRANSFER TRANSITIONS. *Inorganica Chimica Acta* **1992**, *197* (2), 227-232.
8. Schilt, A. A., MIXED LIGAND COMPLEXES OF IRON(II) AND IRON(III) WITH CYANIDE AND AROMATIC DI-IMINES. *J. Am. Chem. Soc.* **1960**, *82* (12), 3000-3005.

9. Terrettaz, S.; Becka, A. M.; Traub, M. J.; Fettinger, J. C.; Miller, C. J., OMEGA-HYDROXYTHIOL MONOLAYERS AT AU ELECTRODES .5. INSULATED ELECTRODE VOLTAMMETRIC STUDIES OF CYANO/BIPYRIDYL IRON COMPLEXES. *J. Phys. Chem.* **1995**, *99* (28), 11216-11224.
10. Wu, J. F.; Alias, M.; de Graaf, C., Controlling the Lifetime of the Triplet MLCT State in Fe(II) Polypyridyl Complexes through Ligand Modification. *Inorganics* **2020**, *8* (2), 17.
11. Zhang, W. K.; Kjaer, K. S.; Alonso-Mori, R.; Bergmann, U.; Chollet, M.; Fredin, L. A.; Hadt, R. G.; Hartsock, R. W.; Harlang, T.; Kroll, T.; Kubicek, K.; Lemke, H. T.; Liang, H. W.; Liu, Y. Z.; Nielsen, M. M.; Persson, P.; Robinson, J. S.; Solomon, E. I.; Sun, Z.; Sokaras, D.; van Driel, T. B.; Weng, T. C.; Zhu, D. L.; Warnmark, K.; Sundstrom, V.; Gaffney, K. J., Manipulating charge transfer excited state relaxation and spin crossover in iron coordination complexes with ligand substitution. *Chem. Sci.* **2017**, *8* (1), 515-523.
12. Zhang, W.; Ji, M.; Sun, Z.; Gaffney, K. J., Dynamics of Solvent-Mediated Electron Localization in Electronically Excited Hexacyanoferrate(III). *J. Am. Chem. Soc.* **2012**, *134* (5), 2581-2588.
13. Bowman, D. N.; Blew, J. H.; Tsuchiya, T.; Jakubikova, E., Elucidating Band-Selective Sensitization in Iron(II) Polypyridine-TiO<sub>2</sub> Assemblies. *Inorganic Chemistry* **2013**, *52* (15), 8621-8628.
14. Ferrere, S., New photosensitizers based upon Fe(L)(2)(CN)(2) and Fe(L)(3) (L = substituted 2,2'-bipyridine): Yields for then photosensitization of TiO<sub>2</sub> and effects on the band selectivity. *Chem. Mat.* **2000**, *12* (4), 1083-1089.
15. Ferrere, S., New photosensitizers based upon Fe-II(L)(2)(CN)(2) and (FeL3)-L-II, where L is substituted 2,2'-bipyridine. *Inorganica Chimica Acta* **2002**, *329*, 79-92.
16. Yang, M.; Thompson, D. W.; Meyer, G. J., Dual pathways for TiO<sub>2</sub> sensitization by Na-2 Fe(bpy)(CN)<sub>4</sub>. *Inorganic Chemistry* **2000**, *39* (17), 3738-+.
17. Ashley, D. C.; Jakubikova, E., Ironing out the photochemical and spin-crossover behavior of Fe(II) coordination compounds with computational chemistry. *Coord. Chem. Rev.* **2017**, *337*, 97-111.
18. Bowman, D. N.; Jakubikova, E., Low-Spin versus High-Spin Ground State in Pseudo-Octahedral Iron Complexes. *Inorganic Chemistry* **2012**, *51* (11), 6011-6019.
19. Machan, C. W.; Adelhardt, M.; Sarjeant, A. A.; Stern, C. L.; Sutter, J.; Meyer, K.; Mirkin, C. A., One-Pot Synthesis of an Fe(II) Bis-Terpyridine Complex with Allosterically Regulated Electronic Properties. *J. Am. Chem. Soc.* **2012**, *134* (41), 16921-16924.
20. Pelascini, F.; Wesolek, M.; Peruch, F.; De Cian, A.; Kyritsakas, N.; Lutz, P. J.; Kress, J., Iron complexes of terdentate nitrogen ligands: formation and X-ray structure of three new dicationic complexes. *Polyhedron* **2004**, *23* (18), 3193-3199.
21. Priimov, G. U.; Moore, P.; Maritim, P. K.; Butalanyi, P. K.; Alcock, N. W., Synthesis of two covalently linked bis(2,2':6',2''-terpyridine) (terpy) chelating ligands with different length spacers, comparison of the crystal structures of their mononuclear nickel(II) complexes, and kinetic and mechanistic studies of the reaction of one ligand with Fe(terpy)(2) (2+). *J. Chem. Soc.-Dalton Trans.* **2000**, (4), 445-449.
22. Rapenne, G.; Dietrich-Buchecker, C.; Sauvage, J. P., Copper(I)- or iron(II)-templated synthesis of molecular knots containing two tetrahedral or octahedral coordination sites. *J. Am. Chem. Soc.* **1999**, *121* (5), 994-1001.
23. Rapenne, G.; Patterson, B. T.; Sauvage, J. P.; Keene, F. R., Resolution, X-ray structure and absolute configuration of a double-stranded helical diiron(II) bis(terpyridine) complex. *Chem. Commun.* **1999**, (18), 1853-1854.
24. Carey, M. C.; Adelman, S. L.; McCusker, J. K., Insights into the excited state dynamics of Fe(II) polypyridyl complexes from variable-temperature ultrafast spectroscopy. *Chem. Sci.* **2019**, *10* (1), 134-144.
25. Kunnus, K.; Li, L.; Titus, C.; Lee, S. J.; Reinhard, M. E.; Koroidov, S.; Kjaer, K. S.; Hong, K.; Ledbetter, K.; Doriese, W. B.; O'Neil, G. C.; Swetz, D. S.; Ullom, J.; Li, D.; Irwin, K.; Nordlund, D.; Cordones, A.; Gaffney, K. J., Chemical control of competing electron transfer pathways in iron tetracyano-polypyridyl photosensitizers. *Chem. Sci.* **2020**, *11* (17), 4360-4373.
26. Sun, Q.; Mosquera-Vazquez, S.; Daku, L. M. L.; Guenee, L.; Goodwin, H. A.; Vauthey, E.; Hausert, A., Experimental Evidence of Ultrafast Quenching of the (MLCT)-M-3 Luminescence in Ruthenium(II) Tris-bipyridyl Complexes via a (3)dd State. *J. Am. Chem. Soc.* **2013**, *135* (37), 13660-13663.
27. Winkler, J. R.; Sutin, N., LIFETIMES AND SPECTRA OF THE EXCITED-STATES OF CIS-DICYANOBIS(2,2'-BIPYRIDINE)IRON(II) AND CIS-DICYANOBIS(2,2'-BIPYRIDINE)RUTHENIUM(II) IN SOLUTION. *Inorganic Chemistry* **1987**, *26* (2), 220-221.
28. Figard, J. E.; Petersen, J. D., PHOTOCHEMISTRY OF PENTACYANOFERRATE(II) COMPLEXES CONTAINING AROMATIC NITROGEN HETEROCYCLIC LIGANDS. *Inorganic Chemistry* **1978**, *17* (4), 1059-1063.
29. Chabera, P.; Kjaer, K. S.; Prakash, O.; Honarfar, A.; Liu, Y. Z.; Fredin, L. A.; Harlang, T. C. B.; Lidin, S.; Uhlig, J.; Sundstrom, V.; Lomoth, R.; Persson, P.; Warnmark, K., Fe-II Hexa N-Heterocyclic Carbene Complex with a 528 ps Metal-to-Ligand Charge-Transfer Excited-State Lifetime. *J. Phys. Chem. Lett.* **2018**, *9* (3), 459-463.
30. Nance, J.; Bowman, D. N.; Mukherjee, S.; Kelley, C. T.; Jakubikove, E., Insights into the Spin-State Transitions in Fe(tpy)(2) (2+): Importance of the Terpyridine Rocking Motion. *Inorganic Chemistry* **2015**, *54* (23), 11259-11268.
31. Vanko, G.; Bordage, A.; Papai, M.; Haldrup, K.; Glatzel, P.; March, A. M.; Doumy, G.; Britz, A.; Galler, A.; Assefa, T.; Cabaret, D.; Juhin, A.; van Driel, T. B.; Kjaer, K. S.; Dohn, A.; Moller, K. B.; Lemke, H. T.; Gallo, E.; Rovezzi, M.; Nemeth, Z.; Rozsalyi, E.; Rozgonyi, T.; Uhlig, J.; Sundstrom, V.; Nielsen, M. M.; Young, L.; Southworth, S. H.; Bressler, C.; Gawelda, W., Detailed Characterization of a Nanosecond-Lived Excited State: X-ray and Theoretical Investigation of the Quintet State in Photoexcited Fe(terpy)(2) (2+). *Journal of Physical Chemistry C* **2015**, *119* (11), 5888-5902.